Cement and Concrete Research 39 (2009) 868–875

Contents lists available at ScienceDirect

Cement and Concrete Research

journal homepage: http://ees.elsevier.com/CEMCON/default.asp

Measuring the change in ultrasonic p-wave energy transmitted in fresh mortar with additives to monitor the setting

Nicolas Robeyst [a,*], Christian U. Grosse [b], Nele De Belie [a]

[a] Magnel Laboratory for Concrete Research, Ghent University, Department of Structural Engineering, Technologiepark Zwijnaarde 904, B-9052 Gent, Belgium
[b] Material Testing Institute, Stuttgart University, Department of Non-Destructive Testing and Monitoring, Pfaffenwaldring 4, D-70550 Stuttgart, Germany

ARTICLE INFO

Article history:
Received 14 January 2009
Accepted 12 June 2009

Keywords:
Ultrasonic
Fresh concrete (A)
Granulated blast-furnace slag (D)
Fly ash (D)
Admixture (D)

ABSTRACT

Research on ultrasonic methods to monitor the setting of concrete has mainly focussed on the wave velocity as a useful quantity. To investigate the application of also the wave energy as a parameter, an experimental program was set up to apply the ultrasonic wave transmission technique on several mortar samples containing air entrainer, blast-furnace slag or fly ash causing clearly different setting behaviour.
The increase of the relative energy E/E_{ref} during setting is generally retarded if ordinary Portland cement is replaced by blast-furnace slag or fly ash. The mixtures with cement of a lower strength class or with large air content were difficult to test with the energy measurements since they were more sensitive to poor sensor contact due to shrinkage. For the other samples, the thresholds $E/E_{ref} = 0.02$ and 0.13 are proposed to easily determine respectively initial and final setting based on the ultrasonic energy measurements.

1. Introduction

The propagation of ultrasonic waves in fresh concrete or mortar is studied for several purposes such as general quality control, determination of the water-to-cement ratio [1] and monitoring of the setting [2–4]. Research on ultrasonic monitoring of setting has mainly focussed on the change of wave velocity in time as a useful quantity, while the wave energy transmission might be equally or better suited since it considers the entire received signal. Moreover, the calculation of wave energy does not require an accurate onset determination of the received signal and therefore is a more unambiguous parameter. However, compared to the ultrasonic velocity, which mainly depends on the density and compressibility of the medium, the energy loss is caused by many other factors [5].

As a wave propagates through a medium its energy decreases with path length due to divergence and attenuation. Divergence, also called geometric attenuation or beam spreading, is the phenomenon by which the amplitude of the wave decreases as the wave front spreads out over a larger area and only depends on the type of wave front and the distance between the sensors in the measurement set-up. Attenuation on the other hand depends on the medium and is much more complex in this case. Fresh concrete is a liquid suspension of different particle types (cement, sand, aggregates and air inclusions) transforming into a porous solid medium by cement hydration reactions [6]. The material attenuation mechanisms can be classified as either absorption or scattering [7]. According to Aggelis et al. [6] scattering is the dominant attenuation mechanism in fresh mortar for high frequencies (>300 kHz) since both sand content and grain size influence the attenuation in this range. Aggelis et al. observed a linear increase of the attenuation in function of the sand content and the slope of this curve was steeper for higher frequencies. However, at low frequencies the wave length is larger than the grain size of the sand and thus the scattering is limited. For example, a fresh mortar with sand 0/4 and an initial p-wave velocity of 500 m/s [8], appears homogeneous for waves with frequencies lower than 500 m/s/0.004 m = 125 kHz [9]. Therefore, the attenuation in the low frequency range is mostly attributed to the presence of air bubbles in the fresh mixture. No matter how sufficient the compaction might be, there is always an amount of entrapped air that varies from 1 to 10%. According to Aggelis [6], air inclusions cause a large attenuation in water for frequencies lower than 100 kHz, but their effect is negligible when they are surrounded by a solid matrix. In fresh mortar however several researchers [8,10–12] observed a low initial velocity attributed to the presence of air which probably also influences the attenuation at early age.

Besides divergence and attenuation, wave energy loss can also be caused by decoupling of the sensors from the hydrating cementitious sample due to shrinkage of the cement matrix. In this case, an air gap exists between the sensor and the sample so that the ultrasonic wave is partly reflected at the sensor-to-air and air-to-sample interface due to the difference in acoustic impedance of these media. The acoustic impedance Z (Pa s/m) of a medium can be calculated with Eq. (1) as shown in Table 1 for some materials [9,13].

$$Z = \rho \cdot v_p \tag{1}$$

where ρ is the density (kg/m³) and v_p is the p-wave velocity (m/s) for that material. At the interface, the energy of the transmitted wave

* Corresponding author. Tel.: +32 9 264 55 39; fax: +32 9 264 58 45.
E-mail address: Nicolas.Robeyst@UGent.be (N. Robeyst).

0008-8846/$ – see front matter © 2009 Elsevier Ltd. All rights reserved.
doi:10.1016/j.cemconres.2009.06.016

Table 1
Density (kg/m³), p-wave velocity (m/s), acoustic impedance (Pa s/m) and absorption (dB/m) of several materials.

Material	Density	P-wave velocity	Acoustic impedance	Absorption (and scattering[b])		
				at 10 kHz	at 50 kHz	at 100 kHz
Air	1.205	343	413 [9]	0.16	1.66	3.28[c]
Water	1000	1480	$1.48 \cdot 10^6$ [9]	$0.02 \cdot 10^{-3}$	$0.58 \cdot 10^{-3}$	$2.34 \cdot 10^{-3}$ [30]
Glycerine (couplant)	1260	1920	$2.42 \cdot 10^6$ [13]	–	–	–
Plastic (nylon)	1120	2600	$2.90 \cdot 10^6$ [31]	–	–	–
Mortar (hardened)[a]	2300	3000–4200	$6.9–9.7 \cdot 10^6$	40	150	180 [32]
Concrete (hardened)[a]	2400	3000–4500	$7.2–10.8 \cdot 10^6$ [9]	40	120	180 [32]

[a] Values may differ depending on the mixture composition.
[b] For heterogeneous materials such as mortar and concrete, absorption and scattering cannot be completely separated.
[c] Calculated according to ISO 9613-1:1993.

depends on the intensity transmission coefficient and is given by Eq. (2) for normal incidence [13].

$$T_n = \frac{4 \cdot Z_1 \cdot Z_2}{(Z_2 + Z_1)^2} \tag{2}$$

where Z_1 and Z_2 are the acoustic impedances of mediums 1 and 2 respectively.

However, when a layer of finite thickness is formed between two media, the intensity transmission coefficient becomes different from Eq. (2) and depends of the ratio of the layer thickness to the ultrasonic wavelength due to the multiple reflections at the two interfaces of the layer [14]. For very thin layers with acoustic impedance smaller than the surrounding media the transmission coefficient is given by Eq. (3).

$$T_n = \frac{4}{\left(\frac{2 \cdot Z_1 \cdot Z_3 + Z_1^2 + Z_3^2}{Z_1 \cdot Z_3}\right) + Z_1 \cdot Z_3 \cdot \left(\frac{k_2 \cdot d}{Z_2}\right)^2} \tag{3}$$

with Z_1, Z_2 and Z_3 the acoustic impedances of the three media ($Z_2 < Z_1$ and Z_3), d the thickness of the thin layer and k_2 the wave number in this layer (medium 2).

If the sensor is protected by a plastic wear cap, the air layer ($Z_2 = 413$ Pa s/m) arises between plastic ($Z_1 = 2.90$ MPa s/m) and mortar ($Z_3 = 8.3$ MPa s/m). Taking into account an air gap width of 1 μm, the transmission coefficient amounts to 0.03 for a frequency of 50 kHz ($k_2 \cdot d = 0.000916$). Thus, due to the large impedance mismatch between air and mortar, only a small fraction of the incident wave is transmitted at the interface. Although the sensor will never entirely detach, this underlines the important influence of sample shrinkage on the energy measurements.

2. Materials and methods

2.1. Mortar mixtures

The ultrasonic measurements were performed on four series of mortar mixtures. Besides ordinary Portland cement (OPC), these mixtures also contained cement replacing additives such as blast-furnace slag (BFS) and fly ash (FA). In the first series of mortar mixtures BFS was added as a separate component to partially replace the cement (30, 50, 70 and 85%). The second series of mortar compositions were made with OPC and different types of blast-furnace cements, in which BFS is merged during the production process. According to EN 197-1, CEM III/A contains 36–65% BFS by mass, CEM III/B 66–80% and CEM III/C 81–95%. In the third series 0, 35, 50 and 67% of the OPC was replaced by FA. Finally, also mortar mixtures were tested in which air entrainer was added in different amounts (1 ml and 2 ml). The standard mortar samples consisted of 1350 g standard sand, 450 g cement and 225 g water and were mixed according to EN 196-1. The chemical composition and the specific surface area of the different cement types and of the additives BFS and FA are given in Table 2.

2.2. Ultrasonic wave transmission measurements

The ultrasonic p-wave transmission measurements on the hardening mortar samples were performed with the FreshCon system developed at the University of Stuttgart. A detailed drawing of the sample cell is given by Reinhardt and Grosse [15]. Every 5 min, a pulse signal with a width of 2.5 μs and thus a frequency band of approximately 400 kHz was generated and transmitted through the fresh mortar with the aid of a piezoelectric broadband transmitter. After traveling through the hardening sample, the signal was received by the ultrasonic receiver and sent to the DAQ card. More details about the FreshCon system are described in previous publications [3,15]. The ultrasonic energy is determined by numerical integration of the squared amplitude values following the onset time. This value is then divided by the reference energy to eliminate the energy loss due to divergence and reflection at the contact interfaces shown in Fig. 1 (sensor-couplant and couplant-plastic). The reference energy was measured during the calibration of the set-up with the container filled with water, but with the same path length. The reflection at the plastic–mortar interface changes in time as the mortar sets so it cannot be completely eliminated.

All the tests were conducted in a climate chamber at 20 °C and 60% relative humidity. During the setting and hardening process, cementitious material tends to shrink due to loss of water caused by evaporation (drying shrinkage) and consumption in hydration reactions (autogenous shrinkage). As mentioned above, this can

Table 2
Chemical composition (%), mineralogical composition according to the Bogue calculation (%) and Blaine specific surface area (m^2/kg) of the cement and the blast-furnace slag.

Cement type	CEM I 52.5	BFS	FA[a]	CEM I 42.5	CEM III/A 42.5	CEM III/B 42.5	CEM III/A 32.5	CEM III/C 32.5
CaO	62.21	40.38	3.21	63.13	51.88	45.17	49.85	43.66
SiO_2	18.84	34.35	53.58	21.22	25.15	28.78	26.88	31.55
Al_2O_3	5.39	11.36	26.49	3.90	7.39	8.89	8.30	9.42
Fe_2O_3	3.79	0.48	7.01	5.05	2.32	1.55	2.01	0.83
MgO	0.86	7.57	2.08	0.89	4	5.80	4.22	4.22
SO_3	3.06	1.65	–	1.70	3.29	3.33	2.97	2.07
CO_2	0.72	0.25	–	0.39	1.17	1.83	1.16	0.97
Cl^-	0.04	0.013	–	0.01	0.04	0.04	0.04	0.22
C_3S	59.6	–	–	57.4	–	–	–	–
C_2S	9.1	–	–	17.6	–	–	–	–
C_3A	7.9	–	–	1.8	–	–	–	–
C_4AF	11.5	–	–	15.4	–	–	–	–
Blaine SSA	370	400	275	315	485	450	345	317

[a] Mean chemical composition of 2 batches.

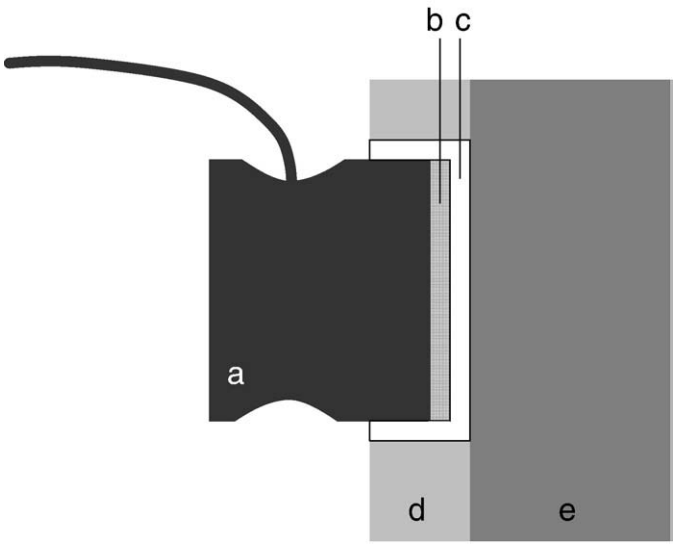

Fig. 1. Schematic representation of the set-up with (a) sensor, (b) couplant, (c) protective wear cap, (d) sample container wall and (e) mortar sample.

lead to a poor contact between the sensors and the sample and consequently severe energy loss. Therefore, the tested mortar was frequently sprinkled with water and the container was sealed with plastic tape to limit the drying shrinkage. Since autogenous shrinkage is mainly important for mixtures with low water-to-cement ratios (<0.42 [16]), its effect on the measurements is expected to be negligible. According to the model of Lee et al. [17] the autogenous shrinkage in concrete with OPC and w/c = 0.5 is limited to $20 \cdot 10^{-6}$ at 48 h. Fig. 2 illustrates the effect of drying shrinkage on both ultrasonic wave energy and velocity. At the age of 2 days, the wave energy measured on the sample that was neither sealed nor cured was reduced to 28% compared to the sample that was properly cured, while the velocity merely decreased to 98% of this reference. This confirms the larger sensitivity of the energy measurements to sensor decoupling compared to velocity measurements.

To indicate the reproducibility of the ultrasonic measurements, the results of three replicates of the mortar mixture with CEM I 52.5 and w/c = 0.5 are given in Fig. 3. Immediately after mixing, high repeatability errors are expected due to the low signal-to-noise ratio of the early recorded waves and the possible variability in air content and compaction degree of the replicate sample. In the period ranging from 4 to 48 h after mixing, the average repeatability error amounted to 1.5% for the velocity and 5.7% for the energy measurement.

2.3. Determination of initial and final setting times

The setting behaviour was also monitored more traditionally with the penetration resistance test (ASTM C403) on mortar. The initial and final setting times are determined by a penetration resistance of respectively 3.5 MPa (the concrete can no longer be vibrated) and 27.6 MPa (the concrete can carry measurable loads) [18]. According to this standard, the coefficient of variation for the initial and final setting time is respectively 7.1% and 4.7%. Except for the mixture with blast-furnace cement CEM III/B 42.5 (10.6% and 14.1%), the

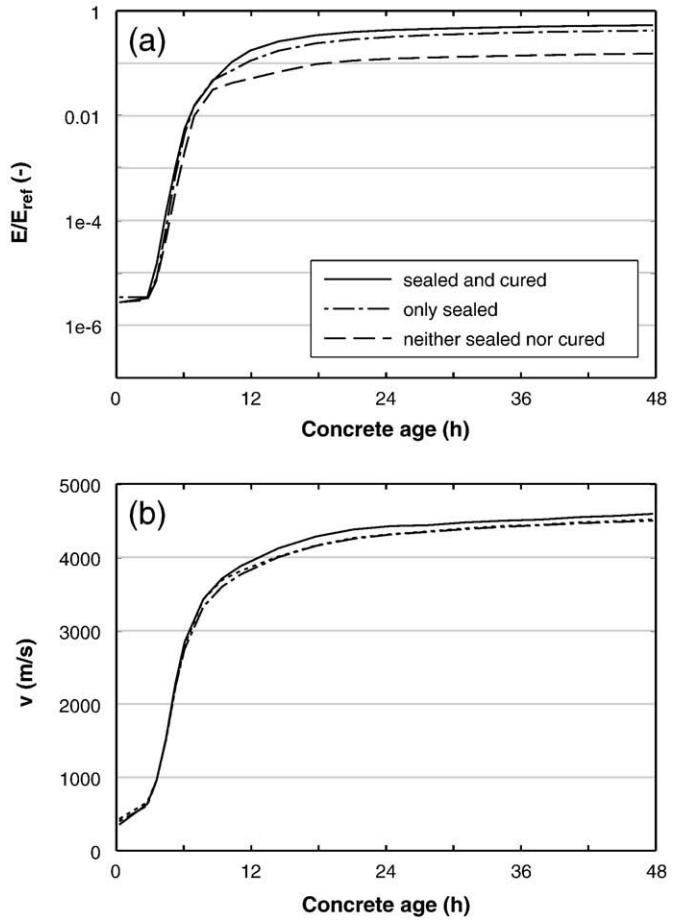

Fig. 2. Effect of sealing and curing the hardening sample during the (a) wave energy and (b) wave velocity measurements (concrete mixture with CEM I 42.5 and w/c = 0.5).

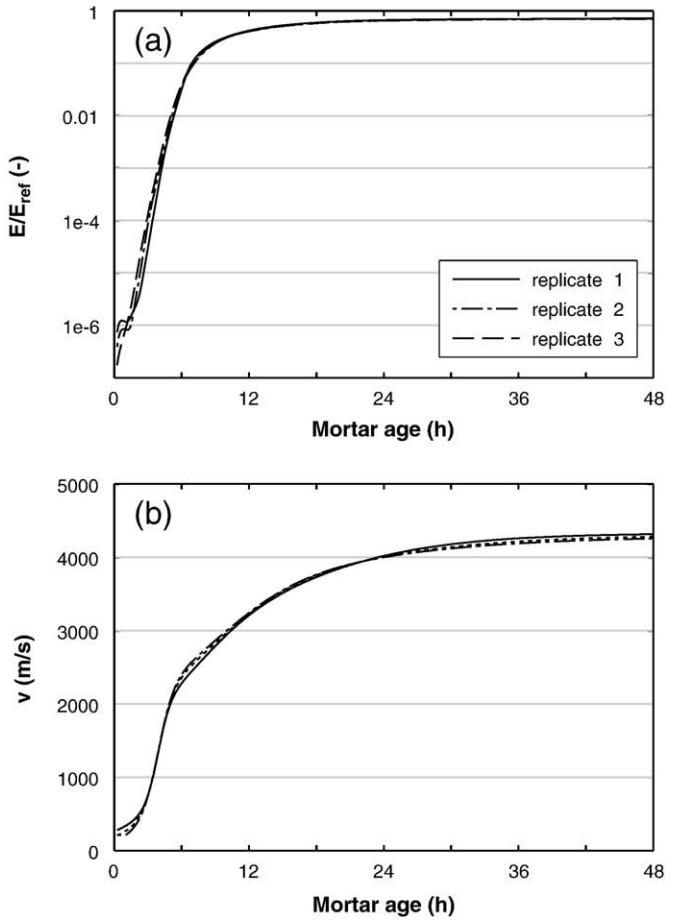

Fig. 3. Ultrasonic (a) wave energy and (b) wave velocity vs. mortar age for three replicates of a properly cured mortar mixture with CEM I 52.5 and w/c = 0.5.

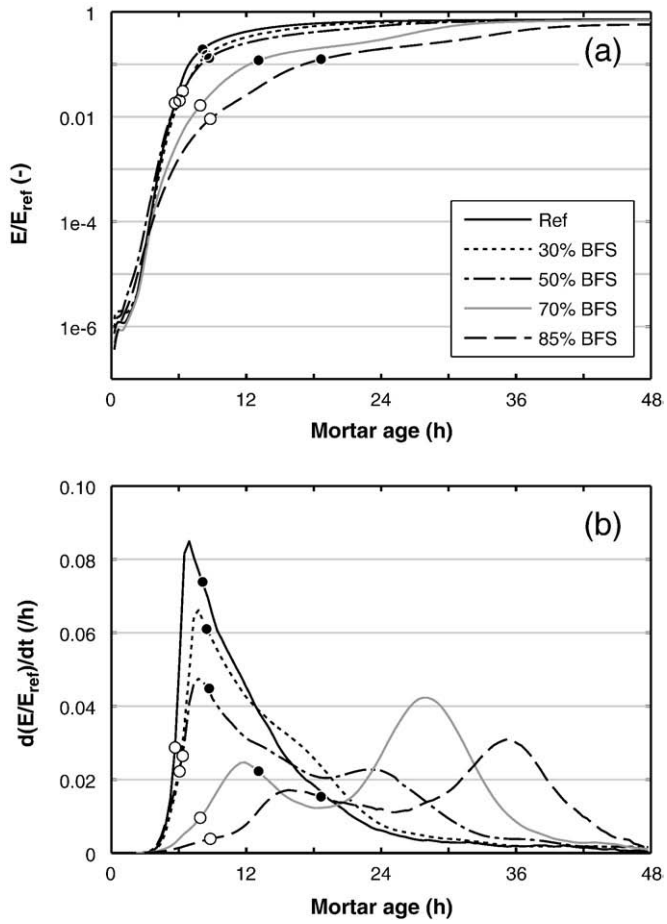

Fig. 4. (a) Ultrasonic energy and (b) its derivative vs. mortar age for standard mortar mixtures in which an increasing percentage of the OPC (CEM I 52.5) was replaced by BFS. The initial and final setting according to ASTM C403 are indicated with white and black dots respectively.

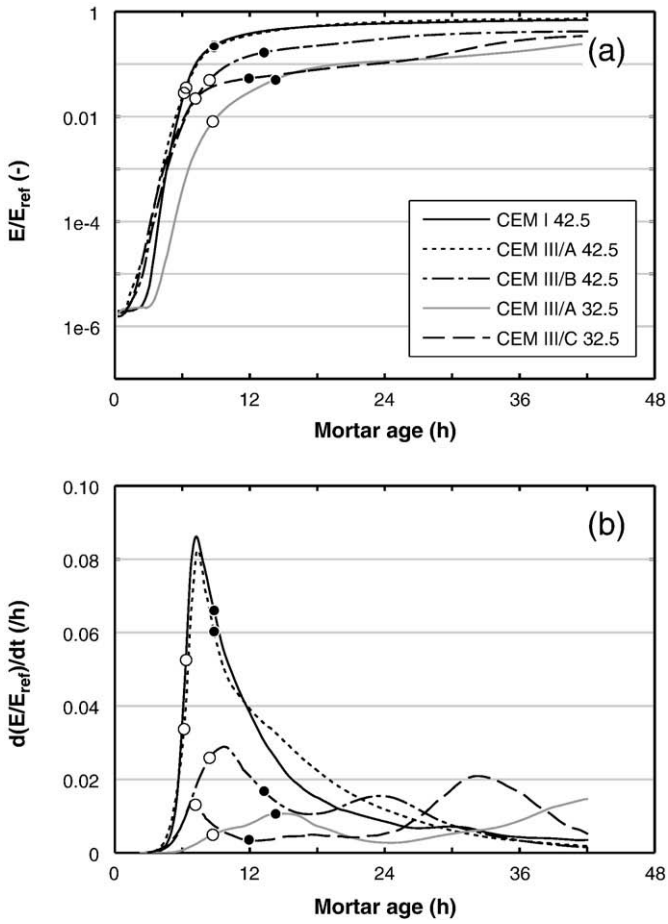

Fig. 5. (a) Ultrasonic energy and (b) its derivative vs. mortar age for standard mortar mixtures with OPC and 4 different blast-furnace cement types. The initial and final setting according to ASTM C403 are indicated with white and black dots respectively.

coefficients of variation of the performed measurements were smaller than these values.

2.4. Semi-adiabatic calorimetric measurements

From every mixture, tested in the FreshCon system, a sample was put in a semi-adiabatic calorimeter (Langavant calorimeter) so ultrasonic and calorimetric measurements were conducted simultaneously. According to the semi-adiabatic method, the temperature rise of the hydrating sample in a heat-insulated flask is continuously measured. The cumulative heat production Q_j at time point j is then calculated with the following formula (EN 196-9):

$$Q_j = \frac{c}{m_c} \cdot \theta_j + \frac{1}{m_c} \cdot \sum_{i=1}^{j} \overline{\alpha}_i \cdot \overline{\theta}_i \cdot \Delta t_i \quad (4)$$

where c is the thermal capacity of the setup, m_c the mass of cement, θ the temperature rise and $\overline{\alpha}_i$ and $\overline{\theta}_i$ the mean coefficient of heat loss and the mean temperature rise of the test sample during period Δt_i between two temperature measurements.

The temperature rise during the semi-adiabatic measurements can amount to 35 °C accelerating the hydration reactions; while the sample in the FreshCon container hydrates under almost isothermal conditions (the temperature increases less than 2 °C). To compare the results of the calorimeter with the ultrasonic measurements, the heat production rate will be shown as a function of the equivalent age at 20 °C, calculated with the maturity function according to the Arrhenius law. The activation energy was set to the value of OPC, namely 33.5 kJ/mol [19] for all mixtures. Although the activation energy of BFS or FA is much higher, this difference was not taken into account because of the difficulties in separating the different reactions.

3. Results and discussion

3.1. Energy measurements

The change of the received ultrasonic wave energy in time and its derivative during the setting of the mortar are given in Figs. 4–7 for the different series. Since the wave energy is calculated as the sum of the squared amplitudes and thus increases rapidly, it is presented on a logarithmic scale capturing the early–age increase. At 48 h the relative wave energy measured on the reference (CEM I 52.5) reached a value of 0.72, which means that the energy received on the reference mortar sample is 72% of the energy received when the container is filled with water. Considering the difference in absorption between water and mortar (Table 1), the wave energy measured on a mortar sample should theoretically be between 0.40 and 0.82 for the range of 10–100 kHz.

The dormant period, during which the wave energy does not increase, is very limited (at the maximum 2 h) or even missing. However, like the early increase of the p-wave velocity [8] this is also caused by other factors than by setting of the cement. In a small experiment performed on standard mortar in which the cement was replaced by non-reactive quartz filler, the energy increased from $1.17 \cdot 10^{-6}$ to $5.19 \cdot 10^{-5}$ during the first 48 h and to $2.71 \cdot 10^{-4}$ after 70 h due to internal settling. Though the effect of the latter seems to be limited, this process will be accelerated in mortar by the cement hydration and coagulation. Also the formation of early hydration

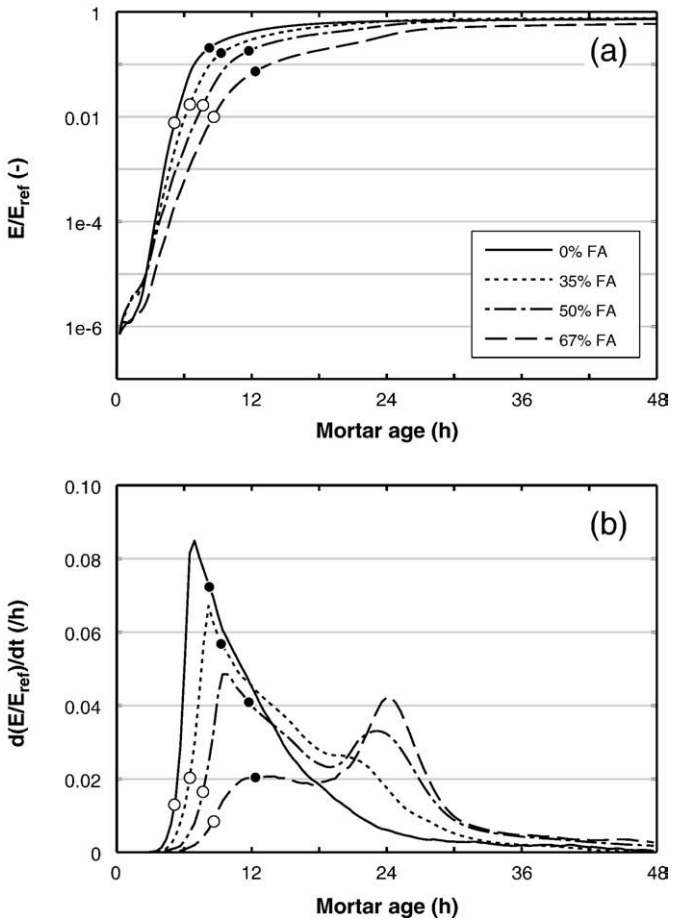

Fig. 6. (a) Ultrasonic energy and (b) its derivative vs. mortar age for standard mortar mixtures in which an increasing percentage of the OPC (CEM I 52.5) was replaced by FA. The initial and final setting according to ASTM C403 are indicated with white and black dots respectively.

products such as ettringite [4] and bleeding [8,20] influence the acoustic characteristics in the beginning.

3.1.1. Mixtures with BFS

Besides the reference sample with only OPC (CEM I 52.5) as binder, mortar in which 30, 50, 70 and 85% of the OPC was replaced by BFS was tested. The change of the received wave energy in time is shown in Fig. 4a for the different mixtures and is similar to that of the wave velocity shown in the previous publication [8]. The hydration of the BFS is not initiated until the lime liberated during the hydration of OPC provides the correct alkalinity [21,22] which causes a slower setting in mixtures with BFS. In mortar with little BFS (30%), the difference with the reference is restricted but clearer compared to the velocity measurements. If a large fraction of the cement is replaced by BFS, the energy curve shows a second increase after approximately 20 h (70% BFS) and 28 h (85% BFS) that might be caused by the slag reaction. The different setting behaviour of the mixtures can even be better distinguished when the derivative of the energy is plotted against mortar age (Fig. 4b). The largest increase in transmitted energy (maximum of the derivative) takes place 8 h after mixing for the reference and the compositions with little BFS. This peak tends to appear at later ages the more OPC is replaced by BFS. Moreover, a second peak becomes visible corresponding to the contribution of the BFS to the setting as mentioned above.

3.1.2. Mixtures with blast-furnace cement

The ultrasonic wave energy and its derivative vs. mortar age for standard mortar mixes with 1 Portland cement (CEM I 42.5) and 4 different types of blast-furnace cement are shown in Fig. 5. Considering the mortars with strength class 42.5, the maximum value at 42 h was reached by the sample with CEM III/A ($E/E_{ref}=0.73$) instead of the OPC mixture ($E/E_{ref}=0.69$) which can be attributed to the higher fineness of the cement type (Table 2). Moreover, the addition of BFS can lead to higher strength and stiffness. The energy curves of these two samples are rather similar. The composition with CEM III/B on the other hand clearly sets slower and the energy merely amounts to $E/E_{ref}=0.42$ after two days.

For the strength class 32.5, the energy increases faster during the first 12–14 h in the mortar made with CEM III/C than in the sample with CEM III/A. This acceleration was also observed in the results of the velocity measurements [8] and was attributed to the higher chloride and lower SO_3 content of CEM III/C in comparison to CEM III/A (Table 2). After a short stagnation, the ultrasonic energy of the mortar containing CEM III/C shows a second acceleration as also noticed in the mixtures with 70% and 85% BFS. However, in both samples of strength class 32.5 only a small fraction of the energy is transmitted at 42 h ($E/E_{ref}=0.25$ and 0.34 respectively). Cement replacing additives such as BFS are known to increase the autogenous shrinkage [17], but this effect is limited for mortar with w/c = 0.5 and at very early age. Moreover, the influence of the BFS on shrinkage and sensor decoupling would also have been observed in the samples with BFS replacement. In addition, cement types with lower values for the Blaine fineness are less sensitive to autogenous shrinkage [23]. However, since these mortar mixtures set slower than the others, they possibly did not adhere enough to the container walls and sensors at early age to prevent decoupling.

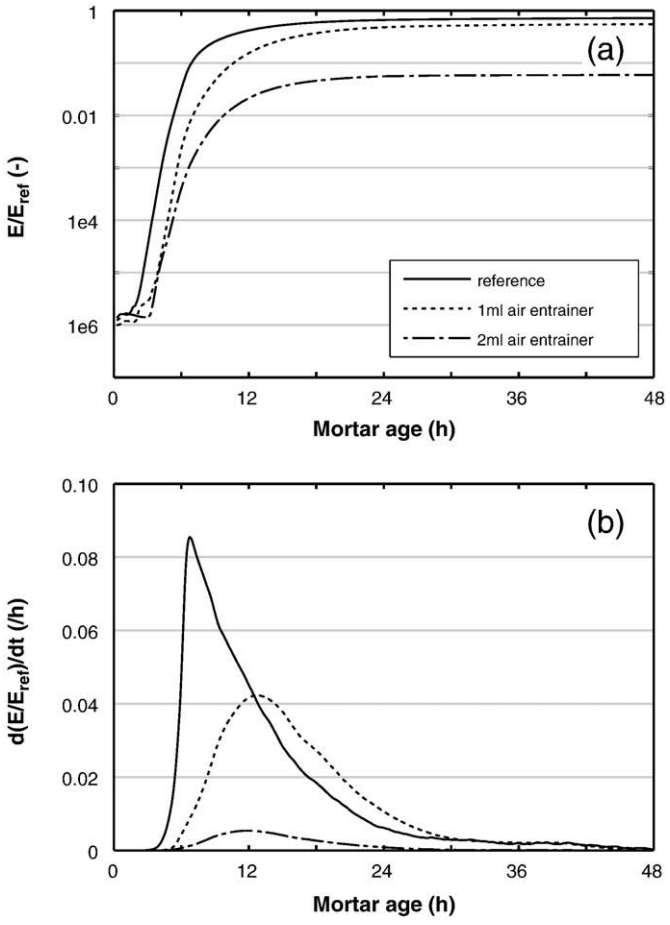

Fig. 7. (a) Ultrasonic energy and (b) its derivative vs. mortar age for standard mortar mixtures in which an increasing amount of air entrainer was added.

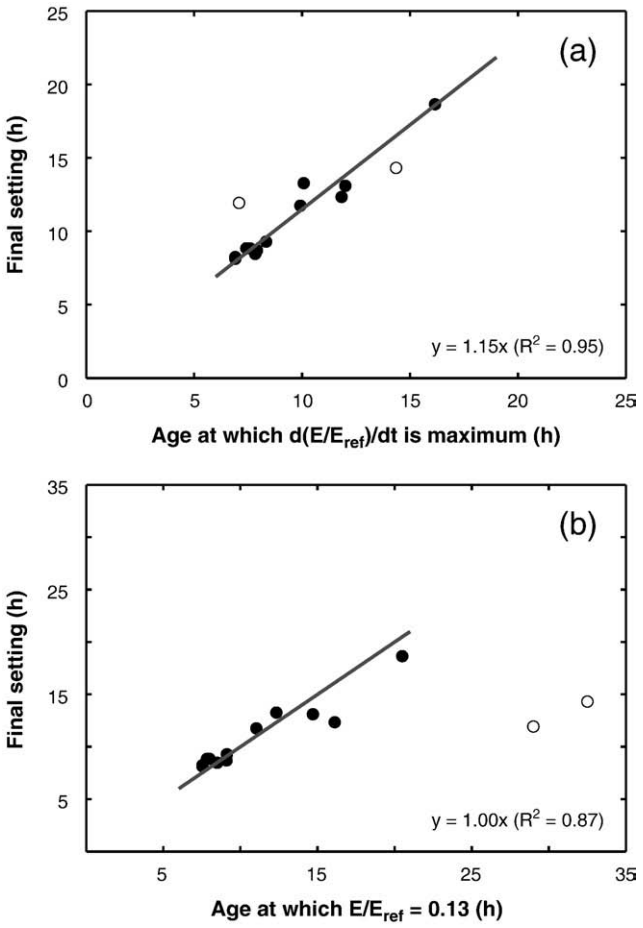

Fig. 8. Correlation between the final setting time (ASTM C403) and the age at which (a) the derivative of the energy $d(E/E_{ref})/dt$ is maximum and (b) the energy reaches a value of $E/E_{ref}=0.13$. The low strength mixtures (CEM III/A 32.5 and CEM III/C 32.5) deviate from the trend and are considered outliers (white dots).

3.1.3. Mixtures with FA

The reference with OPC (CEM I 52.5) is the same as the reference shown above. The other samples contained 35, 50 and 67% FA as binder. Their energy graphs (Fig. 6) resemble those of the mixtures with BFS: a slower increase in the energy and a second peak in the derivative curve when more OPC is replaced by FA. However, the origin of this second peak is less clear and can be the contribution to the setting of reaction products formed by the hydration of FA or by C_3A reactions activated by FA as suggested by Baert et al. [24].

3.1.4. Mixtures with air entrainer

The large influence of the air content of the mixture is illustrated by Fig. 7 in which the measurements on mortar without and with addition of air entrainer are compared. The initial air content (EN 459-2) in the reference was 5.6% while the mortar with addition of 1 ml and 2 ml air entrainer contained respectively 8.7% and 10% air. This difference in initial air content is not reproduced in the initial transmitted energy (Fig. 7a). In the suspension stage 5.6% air seems already sufficient to decrease the transmitted energy to values around 10^{-6} which is not altered by entraining more air. In a previous publication, it was already noticed that the ultrasonic velocity measured shortly after mixing is greatly influenced by little air in the fresh mortar [8].

The change of the energy in time is however clearly influenced by the addition of this chemical admixture. The increase of the transmitted energy was retarded and low values were reached after 48 h, namely $E/E_{ref}=0.55$ and 0.06 when respectively 1 ml and 2 ml air entrainer was added to the mortar. These low values can be caused by the scattering of the ultrasonic waves on air inclusions due to the large impedance mismatch between mortar and air. In addition, although the samples with higher air content will not shrink more, they might be more sensitive to sensor decoupling due to decreased adhesion of the sample to the container walls compared to the reference.

3.2. Comparison between ultrasonic energy and penetration resistance test

In Figs. 4–6 the initial and final setting determined by the penetration resistance test (ASTM C403) are indicated with white and black dots respectively. For most of the samples final setting occurred little after the peak in the derivative curve of the ultrasonic energy. The Pearson correlation between these two time points is 0.97 ($P<0.001$), indicating a linear relation as illustrated in Fig. 8a.

To define a simpler relation between the ultrasonic measurements and the setting times, the relative energy E/E_{ref} reached at initial and final setting according to ASTM C403 was determined for the 14 tested mixtures and their replicates. The mean energy value at final setting amounted to 0.15. However, if a regression was made between the final setting time and the age at which the energy reaches this value, the coefficient in the equation of this line was 0.95 instead of 1. Therefore, Fig. 8b shows the correlation between the final setting time and the age at which $E/E_{ref}=0.13$. Although the Pearson correlation is lower (0.93, $P<0.001$) than with the derivative criterion, the $E/E_{ref}=0.13$ threshold is a more practical criterion for indicating the final setting on the energy curves. The measurements on mortar with lower strength cement (CEM III/A 32.5 and CEM III/C 32.5) deviate from the trend, but since they might be not accurate due to sensor decoupling they are considered outliers. In a similar way, it was determined that the initial setting can be indicated by a threshold value $E/E_{ref}=0.02$. Excluding the samples with the slowest setting behaviour (CEM III/A 32.5 and 85% BFS), the Pearson correlation amounted to 0.89 ($P<0.001$) and the linear relation is shown in Fig. 9. Both criteria are summarized in Eq. (5).

$$\begin{aligned} t_{\text{initial\_set}}(\text{h}) &= t_{E/E_{ref}=0.02}(\text{h}) \\ t_{\text{final\_set}}(\text{h}) &= t_{E/E_{ref}=0.13}(\text{h}) \end{aligned} \tag{5}$$

3.3. Wave energy versus velocity measurements to indicate setting

As illustrated by Fig. 2, the wave velocity approach is less sensitive to sensor coupling and thus to sealing and curing of the sample. However, if a sample is properly cured and sealed, the wave energy approach offers some advantages over the velocity. The calculation of

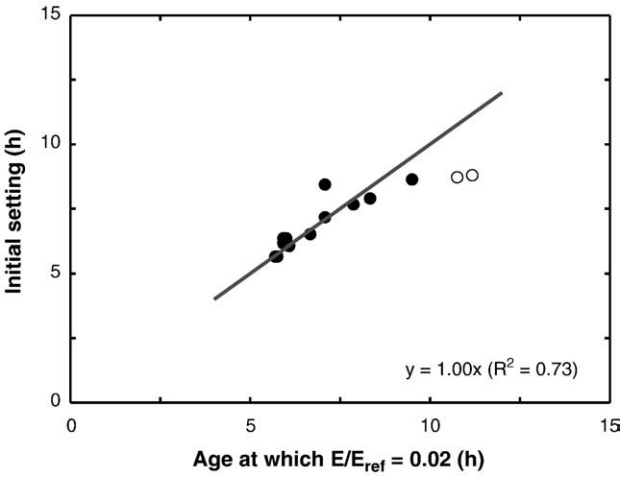

Fig. 9. Correlation between the initial setting time (ASTM C403) and the age at which the energy reaches a value of $E/E_{ref}=0.02$. The slow setting mixtures (CEM III/A 32.5 and 85% BFS) deviate from the trend and are considered outliers (white dots).

the velocity requires an accurate onset determination which can be difficult immediately after mixing due to the poor signal-to-noise ratio. Therefore, the determination of the velocity cannot always be automated the first hours after water addition. Conversely, the calculation of the transmitted energy scarcely relies on the accurate onset determination and is therefore more unambiguous.

In literature, a number of criteria can be found to indicate initial setting based on the wave velocity measurements. Often, a velocity value or range is given to determine the initial setting time: 800–980 m/s (mortar, w/c = 0.27–0.5), 1100–2000 m/s (concrete, w/c = 0.27–0.5) [11], 2300–2700 m/s (concrete, w/c = 0.45–0.6) [25], 1000–1500 m/s (concrete) [26]. Analogously, the final setting is also indicated by a velocity value or range: 1200–1400 m/s (mortar, w/c = 0.27–0.5), 2000–3000 m/s (concrete, w/c = 0.27–0.5) [11], 2790–3180 m/s (concrete, w/c = 0.45–0.6) [25], 3000 m/s (concrete) [26]. On the other hand, also characteristic points in the velocity graph can be useful. According to Robeyst et al. (mortar and concrete) [8], Trtnik et al. (cement paste) [27] and Voigt et al. (mortar and concrete) [4] the inflection point (maximum in the first derivative) indicates the start of the increase in penetration resistance. Robeyst et al. [8] related the final setting to the beginning of the third stage of the velocity curves, namely the slow increase in velocity (time when derivative of the velocity curve has decreased to 20% of its maximum value). Although the criteria based on these characteristic graph points allow an accurate determination of the initial and final setting times, they cannot be used during measurements since they require the entire velocity graph in time. On the other hand, the velocity threshold values vary significantly as demonstrated above, which limits their applicability. Thus, the criteria based on the energy graphs contribute to the study of the setting: they are simple threshold values which can indicate initial and final setting times before the measurements are terminated and this for a variety of mixtures.

Finally, the ultrasonic wave energy can also be used as an indicator whether significant shrinkage has caused sensor decoupling or not. The combined study of both parameters is probably the best approach when using ultrasonic measurements to monitor mortar or concrete setting.

3.4. Semi-adiabatic calorimetric measurements

With the semi-adiabatic calorimeter the heat production is determined of a mortar sample of the same batch as the sample for the ultrasonic measurements. In this way the hydration process and the setting were monitored simultaneously. For a given water-to-cement ratio, setting can be related to the amount of precipitated hydrates [28] so a comparison between setting and hydration is meaningful.

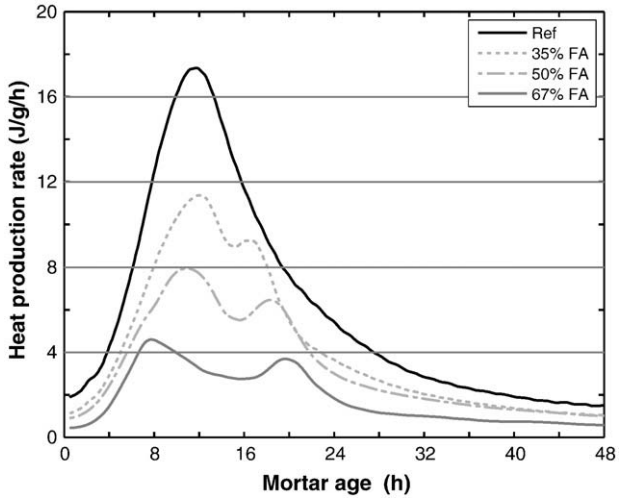

Fig. 10. The heat production rate q (Joule per g binder per h) vs. equivalent mortar age (20 °C) for standard mortar mixtures in which an increasing percentage of the Portland cement was replaced by fly ash.

The heat production of the mortar compositions with BFS and blast-furnace cement are already published in a previous publication [8]. Therefore, Fig. 10 shows the heat production rate q of mortar with an increasing amount of FA under semi-adiabatic conditions, in function of the equivalent age at 20 °C. This quantity is expressed by mass of total binder. Since the mixing occurred outside the calorimeter, the first peak in the evolution of q has been left out.

The similarity between the heat production rate and the derivative of the energy change is the one peak in case of OPC mixtures and the growing second peak the more OPC is replaced by FA. There are however clear differences. The heat production peak due to the rapid hydration of C_3S occurred earlier for the 67% FA mixture. The fly ash particles dispersed in the cement paste act as nucleation sites for the precipitation of hydration products and stimulate the early hydration [29]. This shift of the first maximum is not observed in this direction in the derivative of the energy. At early age, the dispersed fly ash particles do not react themselves and decelerate the initial setting by increasing the distance between the hydrating cement grains. For the FA mortar the second peak in both the heat production and the energy derivative might be caused by the hydration of FA or more likely by C_3A reactions activated by FA [24]. However, the age at which the two peaks occurred in the heat production rate does not correspond with the energy measurements. This can be expected since the setting times depend more on the water-to-cement ratio than the hydration. Moreover, the conversion of the semi-adiabatic hydration rate in time to equivalent age is merely approximate in case of mineral additions. Nonetheless, the similarities between the calorimetric and ultrasonic measurements support the hypothesis that the second increase in the energy curve is caused by reactions activated by the FA. Similarly, this applies to the BFS and blast-furnace cement mixtures, where the second peak in the energy curves is caused by the reaction of the BFS itself.

4. Conclusions

Besides the change of the wave velocity in time, also the wave energy transmission is a useful quantity to monitor the setting behaviour of mortar. As main advantage, the ultrasonic energy depends less on an accurate determination of the signal onset time. The tested mortar has to be frequently sprinkled with water and the container sealed with plastic tape to limit the drying shrinkage and anticipate a poor contact between the sample and the sensors.

The increase of the ultrasonic energy during setting is generally retarded if OPC is replaced by BFS or FA. For the mortars containing high percentages of these cement replacing additives a second increase in the energy graph can be detected after approximately 24 h. Mixtures with low strength cement types or with large air content were difficult to test with the ultrasonic energy measurements. For the other samples, the final setting determined by the standard penetration resistance test (ASTM C403) occurs shortly after the peak in the derivative curve of the ultrasonic energy. In addition, the thresholds $E/E_{ref} = 0.02$ and 0.13 are proposed to easily determine respectively initial and final setting based on the ultrasonic energy measurements.

Acknowledgements

As Research Assistant of the Research Foundation — Flanders (FWO — Vlaanderen), the author Nicolas Robeyst wants to thank the foundation for the financial support. The cooperation with ir. Joris Daems within the framework of his Master's thesis is gratefully acknowledged.

References

[1] T.P. Philippidis, D.G. Aggelis, An acousto-ultrasonic approach for the determination of water-to-cement ratio in concrete, Cem. Concr. Res. 33 (4) (2003) 525–538.
[2] R. D'Angelo, T.J. Plona, L.M. Schwartz, P. Coveney, Ultrasonic measurements on hydrating cement slurries : onset of shear wave propagation, Adv. Cem. Based Mater. 2 (1) (1995) 8–14.
[3] C.U. Grosse, H.W. Reinhardt, M. Krüger, R. Beutel, Ultrasonic through-transmission techniques for quality control of concrete during setting and hardening, Advanced Testing of Fresh Cementitious Materials, Stuttgart, 2006.
[4] T. Voigt, C. Grosse, Z. Sun, S.P. Shah, H.W. Reinhardt, Comparison of ultrasonic wave transmission and reflection measurements with P- and S-waves on early age mortar and concrete, Mater. Struct. 38 (282) (2005) 729–738.
[5] V. Stolojanu, A. Prakash, Characterization of slurry systems by ultrasonic techniques, Chem. Eng. J. 84 (3) (2001) 215–222.
[6] D.G. Aggelis, D. Polyzos, T.P. Philippidis, Wave dispersion and attenuation in fresh mortar: theoretical predictions vs. experimental results, J. Mech. Phys. Solids 53 (4) (2005) 857–883.
[7] W. Punurai, J. Jarzynski, J. Qu, J.-Y. Kim, L.J. Jacobs, K.E. Kurtis, Characterization of multi-scale porosity in cement paste by advanced ultrasonic techniques, Cem. Concr. Res. 37 (1) (2007) 38–46.
[8] N. Robeyst, E. Gruyaert, C.U. Grosse, N. De Belie, Monitoring the setting of concrete containing blast-furnace slag by measuring the ultrasonic p-wave velocity, Cem. Concr. Res. 38 (10) (2008) 1169–1176.
[9] N.J. Carino, Stress wave propagation methods, in: N.J. Carino, V.M. Malhotra (Eds.), Handbook on Nondestructive Testing of Concrete, CRC Press Online, 2004.
[10] C.-L. Hwang, D.-H. Shen, The effects of blast-furnace slag and fly ash on the hydration of portland cement, Cem. Concr. Res. 21 (4) (1991) 410–425.
[11] H.K. Lee, K.M. Lee, Y.H. Kim, H. Yim, D.B. Bae, Ultrasonic in-situ monitoring of setting process of high-performance concrete, Cem. Concr. Res. 34 (4) (2004) 631–640.
[12] G. Ye, P. Lura, K. van Breugel, A.L.A. Fraaij, Study on the development of the microstructure in cement-based materials by means of numerical simulation and ultrasonic pulse velocity measurement, Cem. Concr. Compos. 26 (5) (2004) 491–497.
[13] Y. Kim, S.J. Song, S.S. Lee, J.K. Lee, S.S. Hong, A study on the couplant effects in contact ultrasonic testing, 10th Asia-Pacific Conference on Non-destructive Testing, Brisbane, 2001.
[14] J.L. Rose, P.A. Meyer, Ultrasonic signal-processing concepts for measuring the thickness of thin layer, Mater. Eval. 32 (2) (1974) 249–255.
[15] H.W. Reinhardt, C.U. Grosse, Continuous monitoring of setting and hardening of mortar and concrete, Constr. Build. Mater. 18 (3) (2004) 145–154.
[16] G.R. de Sensale, A.B. Ribeiro, A. Gonçalves, Effects of RHA on autogenous shrinkage of Portland cement pastes, Cem. Concr. Compos. 30 (10) (2008) 892–897.
[17] K.M. Lee, H.K. Lee, S.H. Lee, G.Y. Kim, Autogenous shrinkage of concrete containing granulated blast-furnace slag, Cem. Concr. Res. 36 (7) (2006) 1279–1285.
[18] L.H. Tuthill, W.A. Cordon, Properties and uses of initially retarded concrete, Proc. Am. Concr. Inst. 52 (2) (1955) 273–286.
[19] G. De Schutter, Hydration and temperature development of concrete made with blast-furnace slag cement, Cem. Concr. Res. 29 (1) (1999) 143–149.
[20] T. Chotard, N. Gimet-Breart, A. Smith, D. Fargeot, J.P. Bonnet, C. Gault, Application of ultrasonic testing to describe the hydration of calcium aluminate cement at the early age, Cem. Concr. Res. 31 (3) (2001) 405–412.
[21] A.M. Neville, Properties of Concrete, Longmen, Essex, 1995.
[22] H. Taylor, Cement Chemistry, Thomas Telford Publishing, London, 1990.
[23] A. Naceri, B. Benia, The effect of fineness of cements and mineral additions on the mechanical response of concrete, Asian J. Civ. Eng. (Building and housing) 7 (3) (2006) 239–248.
[24] G. Baert, S. Hoste, G. De Schutter, N. De Belie, Reactivity of fly ash in cement paste studied by means of thermogravimetry and isothermal calorimetry, J. Therm. Anal. Calorim. (2008) Online.
[25] A. Herb, Indirekte Beobachtung des Erstarrens und Erhärtens von Zementleim, Universität Stuttgart, Stuttgart, Mörtel und Beton mittels Schallwellenausbreitung, 2003.
[26] N.G.B. Van der Winden, Ultrasonic measurement for setting control of concrete, International Workshop on Testing during Concrete Construction, Mainz, 1990.
[27] G. Trtnik, G. Turk, F. Kavcic, V.B. Bosiljkov, Possibilities of using the ultrasonic wave transmission method to estimate initial setting time of cement paste, Cem. Concr. Res. 38 (11) (2008) 1336–1342.
[28] A. Nonat, J.C. Mutin, From hydration to setting, in: A. Nonat, J.C. Mutin (Eds.), Hydration and Setting of Cements, Proc of the international RILEM Workshop, Chapman & Hall, London, 1992, pp. 171–191.
[29] J.I. Escalante-Garcia, J.H. Sharp, Effect of temperature on the hydration of the main clinker phases in portland cements: part II, blended cements, Cem. Concr. Res. 28 (9) (1998) 1259–1274.
[30] M.A. Ainslie, J.G. McColm, A simplified formula for viscous and chemical absorption in sea water, J. Acoust. Soc. Am. 103 (3) (1998) 1671–1672.
[31] A. Selfridge, Approximate material properties in isotropic materials, IEEE Trans. Sonics Ultrason. 32 (3) (1985) 381–384.
[32] T.P. Philippidis, D.G. Aggelis, Experimental study of wave dispersion and attenuation in concrete, Ultrason. 43 (7) (2005) 584–595.